Effects of Nano-Fluids Types, Volume Fraction of Nano-Particles, and Aspect Ratios on Natural Convection Heat Transfer in Right-Angle Triangular Enclosure.

Israa Y. Daood*

Received on: 15/12/2009
Accepted on: 30/6/2010

Abstract

This study investigates natural convection heat transfer and fluid flow characteristic of water based nano-fluids in a right-angle triangular enclosure, where the left vertical wall is insulated, the right inclined wall is cooled, and the horizontal wall is heated by spatially varying temperature. Governing equations are solved using stream-vorticity formulation in curvilinear coordinates. Streamlines, isotherms, local and average Nusselt number, moreover to NUR factor are used to present the corresponding flow and thermal fields inside the triangular enclosure. Calculation were performed for three aspect ratio of enclosure geometry (AR=0.5, 1, 2), solid volume fractions of nano-particles ranging from *PHI*=0, to 4%, and Rayleigh number varying from 10^4 to 10^6. Three types of nano-particles are taken into consideration: Cu, Al_2O_3, and TiO_2. The results show that, the average heat transfer rate increases significantly as particle volume fraction and Rayleigh number increase. Also, the type of nano-fluid is a key factor for heat transfer enhancement where the high values are obtained when using Cu, TiO_2 and Al_2O_3 nano-particles respectively. Finally, it is observed that the aspect ratio of the enclosure is one of the most important on flow and heat transfer. Increasing the AR leads that to increase the flow strength and heat transfer rate.

Keywords: Nano-fluids, laminar flow, heat transfer enhancement, right-angle triangular

تاثيرات نوعية Nano-Fluid نسبة حجم الجزيئات المتناهية الصغر والنسب الباعية للحيز المثلث القائم الزاوية في حالة انتقال الحرارة بالحمل الحر

الخلاصة

الدراسة الحالية بحثت ظاهرة انتقال الحرارة بالحمل الطبيعي وسمات جريان المائع المركب من الماء كمائع أساسي ودقائق متناهية بالصغر كجزء ثانوي داخل حيز مثلث قائم الزاوية, حيث أن الجدار الايسر معزول, الجدار الايمن المائل مبرد, والجدار الأفقي مسخن بتغير حيزي لدرجة الحرارة ($T = f(x)$).المعادلات الحاكمة حُلت بطريقة دالة-الانسياب- الدوامية بأحداثيات مطابقة الجسم. خطوط الأنسياب, خطوط ثبوت درجات الحرارة, ورقم ناسلت الموضعي والمعدل بالأضافة الى العامل NUR أستخدمت لأظهار مجال الجريان وانتقال الحرارة داخل الحيز. الحسابات أخذت لثلاث نسب باعية للشكل الهندسي للحيز (AR=0.5, 1, 2), نسب حجم الدقائق الصلبة المتناهية بالصغر (*PHI*=0, to 4%), و لمدى من رقم رايلي من 10^4 الى 10^6 , الدراسة شملت ثلاث أنواع من الدقائق الصلبة المتناهية بالصغر هي Cu, Al_2O_3, و TiO_2 .

النتائج وضُحت أن معدل أنتقال الحرارة يزداد طبقاً الى زيادة نسب الحجوم ورقم رايلي. كذلك تم أستنتاج بان نوع المائع المحتوي على دقائق متناهية بالصغرهو المفتاح الرئيسي للتحسس أنتقال الحرارة حيث كانت أعلى قيم لذلك في حالة Cu, TiO_2 , Al_2O_3 على الترتيب. أخيراً أستنتج بأن النسب الباعية للحيز هي أحد أهم العوامل المؤثرة على ظاهرة أنتقال الحرارة وحركة المائع, وبزيادتها يؤدي ذلك الى زيادة قوة الجريان ومعدل انتقال الحرارة.

* Mechanical Engineering Department, University of Technology / Baghdad

Introduction

The primary limitation of conventional fluids such as water, ethylene glycol or propylene glycol is their low thermal conductivity. Therefore in recent years nano-fluids have attracted more attention for cooling in various industrial applications. Such fluids consist of suspended nano-particles which have a better suspension stability compared to millimeter or micrometer sized ones. Use of metallic -particles with high thermal conductivity will increase the effective thermal conductivity of these types of fluid remarkably. For instance just 0.3% volume fraction of copper nano-particles with 10 nm diameter led to an increase of up to 40% in the thermal conductivity of ethylene glycol **[1]**, indeed when nanosized particles are added to liquid flow.

Nano-fluids, as a kind of new engineering material consisting of nanometer sized additives and base fluids. Have attracted great attention of investigation for its superior thermal properties and many potential applications. Many investigations on nano-fluids were reported and especially some interesting phenomena. **Yanjiao et. al.,2009 [2]** shows a review of recent development in research on synthesis and characterization of stationary nano-fluids and try to find some challenging issues that need to be solved for future research. **Eiyad, 2009 [3]** studied the heat transfer enhancement in horizontal annuli using variables properties of Al_2O_3-water nano-fluid. It was observed that for $Ra \geq 10^4$, the average Nusselt number was reduced by increasing the volume fraction of nano-particles. Also, the results show that, the difference in Nusselt number between the Maxwell-Garnett and Chon et. al. models prediction is small, but there was a deviation in prediction at $Ra = 10^3$ and this deviation becomes more significant at high volume fraction of nano-particles.

Eiyad et. al., 2009 [4] showed a numerical analysis of the effect of inclination angle on natural convection heat transfer and fluid flow in a two-dimensional enclosure filled with Cu-water nano-fluid. The performance of nano-fluids is tested inside an enclosure by taking into account the solid particle dispersions. The angle of inclination was used as a control parameter for flow and heat transfer, results showed that, percentage of heat transfer enhancement using nano-particles decreases for higher Rayleigh numbers.

Eiyad et. al., 2009 [5] investigated the heat transfer enhancement in differentially heated enclosure using variables thermal conductivity and variable viscosity of Al_2O_3-water and CuO-water nano-fluids. The results are presented over a wide range of Rayleigh number (10^3-10^5), volume fraction of nano-particles ($0 \leq PHI \leq 9\%$), and aspect ratio ($0.5 \leq AR \leq 2$). Results show that, the Nusselt number was not sensitive to the volume fraction at low Rayleigh number but it sensitive to the aspect ratio. Also, they found that, at high Rayleigh number the average Nusselt number was more sensitive to the viscosity models than to the thermal conductivity models.

Elif, 2009 [6] investigate natural convection heat transfer for water based nano-fluids in an inclined square enclosure where the left vertical side is heated with a constant heat flux, the right side is cooled, and the other sides are kept adiabatic. The governing equations are solved using polynomial differential quadrature method. Calculation were performed for inclination angles from 0^o to 90^o, solid volume fractions ranging from 0% to 20%, constant heat flux heaters of lengths 0.25, 0.5 and 1., Rayleigh number varying from 10^4 to 10^6. Five types of nano-particles are taken into consideration Cu, Ag, CuO, Al_2O_3, and TiO2. The results show that, the average heat transfer rate increases

significantly as particle volume fraction and Rayleigh number increases.

Hakan et. al., 2008 [7] studied the heat transfer fluid flow due to buoyancy forces in partially heated enclosure using nano-fluids and different types of nano-particles. The flush mounted heater is located to the left vertical wall with a finite length as shown in figure (1.A). The governing equations are solved using finite volume technique, the calculation were performed for Rayleigh number ($10^3 \le Ra \le 5*10^5$), height of heater ($0.1 \le h \le 0.75$), location of heater ($0.5 \le y_p \le 0.75$), aspect ratio ($0.5 \le AR \le 2$),volume fraction of nano-particles ($0. \le PHI \le 0.2$), and different types of nano-particles were tested. The major results show that, an increase in mean Nusselt number was found with the volume fraction of nano-particles for the whole range of Rayleigh number. **Eiyad et. al., 2008 [8]** demonstrates heat transfer enhancement in horizontal annuli using nano-fluids. Water based nano-fluid containing various fractions of Cu, Ag, Al_2O_3, and TiO_2 nano-particles were used. The addition of different types and different volume fractions of nano-particles were found to have adverse effects on heat transfer characteristics. The results represented that, for high values of Rayleigh number and high aspect ratio, nano-particles with high thermal conductivity case significant enhancement of heat transfer characteristics. On the other hand, for intermediate values of Rayleigh number nano-particles with low thermal conductivity case a reduction in heat transfer. **Ghasem et. al., 2009 [9]** presented the periodic natural convection in an enclosure filled with nano-fluids. Whilst a heat source with oscillating heat flux is located on the left wall of the enclosure, the right wall is maintained at a relatively low temperature and the other walls are thermally insulated. Based upon numerical predictions, the effects of pertinent parameters such as Rayleigh number, solid volume fraction, heat source position, type of nano-particles an oscillation period are examined. A periodic behavior is found for the flow and temperature fields as results of the oscillating heat flux. The results of this study can be used in the design of an effective cooling system for electronic components to help ensure effective and safe operational conditions. In fact, convective heat transfer is affected by the thermophsical properties of the nano-fluid such as viscosity and thermal conductivity. A recent nano-fluids heat transfer study on forced convection conducted by **Mansour et. al., 2007[10]** revealed that for forced convection different expressions for thermo-physical properties of nano-fluids leads to totally different predictions for the performance of system.

Akbari et. al., 2008 [11] studied the laminar mixed convection of a nano-fluid in horizontal and inclined tubes with uniform heat flux. The effect of tube inclinations and nano-particles concentration on the hydrodynamics and thermal parameters for different Reynolds number and Grashof number combinations are shown and discussed. The results show that, heat transfer coefficient increases by 15% at 4% volume fraction of Al_2O_3. **Hwang et. at., 2009 [12]** have measured the pressure drop and convective heat transfer coefficient of water-based Al_2O_3 nano-fluids flowing through a uniformly heated circular tube in the fully developed laminar flow regime. The experimented results show that, the data of nano-fluid friction factor show a good agreement with analytical predications from Darcy's equation for single-phase flow.

Ho et. at., 2009 [13] investigated experimentally forced convection cooling performance of a copper microchannel heat sink with Al_2O_3-water nano-fluid as the coolant. The microchannel heat sink fabricated consists of 25 parallel rectangular microchannels of length 50mm

with a cross sectional area of 383μm in width by 800μm in height for each microchannel. Results demonstrated that, the nano-fluid cooled heat sink outperforms the water-cooled one, having significantly higher average heat transfer coefficient and thereby markedly lower thermal resistance and wall temperature at high pumping power. For laminar flow forced convection heat transfer of Al_2O_3 – water nano-fluid inside a circular tube with constant wall temperature was investigated experimentally by **Heris et. al., 2007 [14].** Experimental results emphasize the enhancement of heat transfer due to the nano-particles presence in the fluid. Also, heat transfer coefficient increases by increasing the concentration of nano-particles in nano-fluid.

Mirmasoumi et. al., 2008 [15] studied numerically of fully developed mixed convection of a nano-fluid Al_2O_3-water. Two phase mixture models has been used to investigate the effects of nano-particles mean diameter on the flow parameters. The calculated results demonstrate that the convection heat transfer coefficient significantly increases with decreasing the nano-particles mean diameter. **Akbarinia et. at., 2007 [16]** worked the same previous study for laminar mixed convection but for horizontal curved tube. Simultaneous effects of the buoyancy force, centrifugal force, and nano-particles concentration has been presented and discussed. The nano-particle volume fraction dose not has a direct effect on the secondary flow, axial velocity and the skin friction coefficient.

Nano-fluids are a new kined of heat transfer fluids containing a small quantity of non-sized particles (usually less than 100 μm) that are uniformly and stably suspended in a liquid. Therefore, the scope of the current research is to present the effects of nano-particles types (Cu, Al_2O_3, TiO_2), volume fraction of nano-particles (PHI=0, 0.1, 0.2, 0.4), aspect ration of the right angle triangular enclosure (AR=0.5, 1, 2), Rayleigh number ($Ra=10^3$ to 10^6) on flow field, temperature distribution and natural convection heat transfer enhancements.

Based on above literature survey and to the Author's knowledge, no previous study takes these parameters on this geometry of the enclosure (right-angle triangular).

Geometrical Description

The proposed physical model for a two-dimension right-angle triangular enclosure (height H, width W) filled with nano-fluid which is Newtonian, incompressible, and laminar as shown in fig. (1.B). The study applied for three types of nano-fluids (Cu-water, Al_2O_3 – water, TiO_2-water), three aspect ratio of the enclosure geometry (AR=0.5, 1, 2), different values of nano-particles volume fraction (PHI=0, 0.1, 0.2, 0.4), for wide range of Rayleigh number ($Ra=10^3$-10^6). The vertical wall of the enclosure assumed to be insulated and the bottom wall considered to be heated wall and spatially varying with sinusoidal temperature T_h as the expression below:

$$T_h(x) = 0.5 \cdot [1 - \cos(2 \cdot p \cdot x)] \quad ...(1)$$

While the other wall kept at cooled temperature T_c .

Governing Equation and Formulation

Figure (1.B) shows a schematic diagram of right-angle triangular enclosure. The fluid in the enclosure is a water-based nano-fluid containing different types of nano-particles such as (Cu, Al_2O_3, TiO_2). It is assumed that the base fluid (water) and nano-particles are in thermal equilibrium and no slip accurse between them. The thermo-physical properties of the nano-fluid are given as shown in Table (1) [7]:

The thermo-physical properties of the nano-fluid are assumed to be constant except for the density variation which is approximation by the Boussinesq model. The governing equations for the laminar

and steady state natural convection in terms of the stream function-vorticity formulation are:

Stream function-vorticity

$$\frac{\partial^2 y}{\partial x^2} + \frac{\partial^2 y}{\partial y^2} = -w \qquad \dots (2)$$

Vorticity

$$\frac{\partial w}{\partial t} + \frac{\partial}{\partial x}(w \cdot \frac{\partial y}{\partial y}) - \frac{\partial}{\partial y}(w \cdot \frac{\partial y}{\partial x}) = \frac{m_{nf}}{r_{nf}}(\frac{\partial^2 y}{\partial x^2} + \frac{\partial^2 y}{\partial y^2}) + F1 \cdot g \cdot \frac{\partial T}{\partial x} \qquad \dots (3)$$

Energy

$$\frac{\partial T}{\partial t} + \frac{\partial}{\partial x}(T \cdot \frac{\partial y}{\partial y}) - \frac{\partial}{\partial y}(T \cdot \frac{\partial y}{\partial x}) = \frac{\partial}{\partial x}(a_{nf} \cdot \frac{\partial T}{\partial y}) + \frac{\partial}{\partial y}(a_{nf} \cdot \frac{\partial T}{\partial x}) \qquad \dots (4)$$

Where

$$F1 = \frac{(PHI \cdot r_s \cdot b_s + (1 - PHI) \cdot r_f \cdot b_f)}{r_{nf}}$$

$$a_{nf} = \frac{k_{nf}}{(r \cdot C_p)_{nf}}$$

The effective density of the nano-fluid is given as:

$$r_{nf} = (1 - PHI) \cdot r_f + PHI \cdot r_s \qquad \dots (5)$$

The heat capacitance of the nano-fluid is expressed as [17, 18]:

$$(r \cdot C_p)_{nf} = (1 - PHI) \cdot (r \cdot C_p)_f + PHI \cdot (r \cdot C_p)_s \qquad \dots (6)$$

The effective thermal conductivity of the nano-fluid is approximated by Maxwell-Garnetts model:

$$\frac{k_{nf}}{k_f} = \frac{k_s + 2k_f - 2 \cdot PHI(k_f - k_s)}{k_s + 2k_f + PHI(k_f - k_s)} \qquad \dots (7)$$

The use of this equation is restricted to spherical nano-particles where it dose not account for other shapes of nano-particles. This model is found to be appropriate for studying heat transfer enhancement using nano-fluids [16, 17]. The viscosity of the nano-fluid can be approximated as viscosity of a base fluid m_f containing dilute suspension of fine spherical particles and is given by [19]:

$$m_{nf} = \frac{m_f}{(1 - PHI)^{2.5}} \qquad \dots (8)$$

The two components of velocities are given by the following relations, respectively:

$$u = \frac{\partial y}{\partial y} \quad , \quad v = -\frac{\partial y}{\partial x} \qquad \dots (9)$$

The following dimensionless groups are introduced:

$$x = \frac{x}{H}, \; y = \frac{y}{H}, \; \Omega = \frac{wH^2}{a}, \; \Psi = \frac{y}{a}, \; V = \frac{vH}{a}$$

$$U = \frac{uH}{a}, \; q = \frac{T - T_c}{T_h - T_c} \qquad \dots (10)$$

By using the dimensionless parameter the equations are written as:

$$\frac{\partial^2 \Psi}{\partial x^2} + \frac{\partial^2 \Psi}{\partial y^2} = -\Omega \qquad \dots (11)$$

$$\frac{\partial \Omega}{\partial t} + \frac{\partial}{\partial x}(\Omega \cdot \frac{\partial \Psi}{\partial y}) - \frac{\partial}{\partial y}(\Omega \cdot \frac{\partial \Psi}{\partial x}) = F2(\frac{\partial^2 \Psi}{\partial x^2} + \frac{\partial^2 \Psi}{\partial y^2}) + F3 \cdot \frac{\partial q}{\partial x} \qquad \dots (12)$$

$$\frac{\partial q}{\partial t} + \frac{\partial}{\partial x}(q \cdot \frac{\partial \Psi}{\partial y}) - \frac{\partial}{\partial y}(q \cdot \frac{\partial \Psi}{\partial x}) = \frac{\partial}{\partial x}(l \cdot \frac{\partial q}{\partial y}) + \frac{\partial}{\partial y}(l \cdot \frac{\partial q}{\partial x}) \qquad \dots (13)$$

Where

$$F2 = \left[\frac{\Pr}{(1 - PHI)^{0.25} \left[(1 - PHI) + PHI \frac{r_s}{r_f} \right]} \right]$$

$$F3 = Ra \cdot \Pr \left[\frac{1}{\frac{(1 - PHI)}{PHI} \frac{r_f}{r_s} + 1} \cdot \frac{b_s}{b_f} + \frac{1}{\frac{PHI}{(1 - PHI)} \cdot \frac{r_f}{r_s} + 1} \right]$$

$$l = \frac{k_{nf}/k_f}{(1-PHI)+PHI\cdot\frac{(r\cdot C_p)_s}{(r\cdot C_p)_f}}$$

The dimensionless boundary conditions are written as:

On the bottom (Heated) wall:

$$\Psi = 0, \Omega = -\frac{\partial^2\Psi}{\partial y^2}, q(x) = 0.5\cdot[1-\cos(2\cdot p\cdot x)]$$

On the vertical wall:

$$\Psi = 0,\ \ \Omega = -\frac{\partial^2\Psi}{\partial x^2},\ \ \frac{\partial q}{\partial x} = 0$$

On the inclined wall:

$$\Psi = 0,\ \ \Omega = -\left[\frac{\partial^2\Psi}{\partial x^2}+\frac{\partial^2\Psi}{\partial y^2}\right],\ \ q = 0$$

Grid Generation

It is of great importance to implement the surrounding boundaries of arbitrary curvature in the governing equations and to become a part of solution. The proper choice of the used technique to transfer the physical domain into computational domain has a great influence on the solution. Elliptical Partial differential equations method is the most general, applicable and programmable method. There are two types of generating system, Laplace equation type and Poisson equation type. The second type was used in this study.

The transformation function $\xi = \xi(x,y),\ \ \eta = \eta(x,y)$ is individually obtained by solving the following two elliptic Poisson equations:

$$\frac{\partial^2 x}{\partial x^2}+\frac{\partial^2 x}{\partial y^2} = P(x,y)$$
$$\frac{\partial^2 h}{\partial x^2}+\frac{\partial^2 h}{\partial y^2} = Q(x,y) \qquad \text{... (14)}$$

Where P and Q are two arbitrary function specified to adjust the local density of the grids. Meanwhile, the orthogonality of the generated grids system can be improved by carefully setting the boundary conditions. Figure (1.C) show symbol of curvilinear grid system applied in this study.

Then, the set of non-dimensional transformed equation are:

$$A\cdot\frac{\partial^2\Psi}{\partial x^2}+2B\cdot\frac{\partial^2\Psi}{\partial x\partial h}+C\cdot\frac{\partial^2\Psi}{\partial h^2}+D\cdot\frac{\partial\Psi}{\partial h}+E\cdot\frac{\partial\Psi}{\partial x} = -J\cdot\Omega \qquad \text{..(15)}$$

$$\frac{\partial\Omega}{\partial t}+\frac{\partial\Psi}{\partial h}\cdot\frac{\partial\Omega}{\partial x}-\frac{\partial\Psi}{\partial x}\cdot\frac{\partial\Omega}{\partial h} = F2\cdot\left[\begin{array}{l} A\cdot\frac{\partial^2\Omega}{\partial x^2}+2B\cdot\frac{\partial^2\Omega}{\partial x\partial h} \\ +C\cdot\frac{\partial^2\Omega}{\partial h^2}+D\cdot\frac{\partial\Omega}{\partial h} \\ +E\cdot\frac{\partial\Omega}{\partial x}\end{array}\right]+ F3\cdot\left[\frac{\partial y}{\partial h}\cdot\frac{\partial q}{\partial x}-\frac{\partial y}{\partial x}\cdot\frac{\partial q}{\partial h}\right] \qquad \text{… (16)}$$

$$\frac{\partial q}{\partial t}+\frac{\partial\Psi}{\partial h}\cdot\frac{\partial q}{\partial x}-\frac{\partial\Psi}{\partial x}\cdot\frac{\partial q}{\partial h} = \left[\begin{array}{l} A\cdot\frac{\partial^2 q}{\partial x^2}+2B\cdot\frac{\partial^2 q}{\partial x\partial h} \\ +C\cdot\frac{\partial^2 q}{\partial h^2}+D\cdot\frac{\partial q}{\partial h} \\ +E\cdot\frac{\partial q}{\partial x}\end{array}\right] \qquad \text{… (17)}$$

Where

$$\bar{a} = \left(\frac{\partial x}{\partial h}\right)^2+\left(\frac{\partial y}{\partial h}\right)^2,\ g = \left(\frac{\partial x}{\partial x}\right)^2+\left(\frac{\partial y}{\partial x}\right)^2$$

$$J = \frac{\partial x}{\partial x}\cdot\frac{\partial y}{\partial h}-\frac{\partial y}{\partial x}\cdot\frac{\partial x}{\partial h}$$

$$s = \frac{\partial x}{\partial x}\cdot\frac{\partial x}{\partial h}+\frac{\partial y}{\partial x}\cdot\frac{\partial y}{\partial h}$$

$$A = \bar{a}/J\ ,\ B = -s/J\ ,\ C = g/J$$

$$D = \frac{\partial B}{\partial x}+\frac{\partial C}{\partial h}\ ,\ E = \frac{\partial A}{\partial x}+\frac{\partial B}{\partial h}$$

And the boundary conditions become:

$$\Psi|_{h=0,1}=0. \quad , \quad \Psi|_{x=0,1}=0.$$

$$q|_{h=0}=0.5\cdot[1-\cos(2\cdot p\cdot x)] \quad , \quad q|_{h=1}=q|_{x=1}=0.$$

$$\left.\frac{\partial q}{\partial h}\right|_{x=0}=0., \Omega|_{h=0,1}=\left.\frac{C}{J}\cdot\frac{\partial^2\Psi}{\partial h^2}\right|_{h=0,1}, \Omega|_{x=0,1}=\left.\frac{C}{J}\cdot\frac{\partial^2\Psi}{\partial x^2}\right|_{x=0,1}$$

Grid Testing and Code Validation

Figure (2) demonstrates the influence of number of grid points for a test case of fluid confined within the present configuration at Ra=10^5, AR=1. , and *PHI*=0. Figure shows the distribution of u, v, and q for point located in the mid sections of the enclosure with grid number, it is clear that, the grid system of $41*41$ is fine enough to obtain accurate results. Therefore, adopted a grid system of $41*41$.

In order to validate the present code, the streamlines and isotherms are calculated as shown in figure (3) for natural convection in a differentially heated enclosure filled with water (Pr=6.2) for case study of [7] as a present in figure (1.A). In this test the enclosure filled with Cu-water nano-fluid with (Ra = 10^5, y_p = 0.5, AR = 1, h = 0.1, *PHI* = 0.1). The present results are in good agreement with results of [7] as shown in figure (3), therefore the numerical procedure is reliable and efficient.

Numerical implementation

The governing equation in the curvilinear coordinates (equations 15, 16, and 17) as well as boundary conditions were discretized by finite difference method. In this study the finite difference equation were derived by using central difference approximation for the partial derivatives except the convective terms for which upwind difference formula was employed. Derivative at the boundary were approximated by three point forward or backward difference. The explicit method was chose for the solution of flow and energy fields, while relaxation method was chose for stream function calculation. A time increment $\Delta t=10^{-5}$ has been used for Ra=10^3-10^5 and 10^{-7} for Ra=10^6.

In order to evaluate how the presence of the nano-fluids affect the heat transfer rate along the hot wall according to the parameters Rayleigh number, nano-particles volume fraction, and aspect ratio it is necessary to observe the variation of the local Nusselt number on the hot wall. In generalized coordinate the local and average Nusslet number defined as:

$$Nu_l=\frac{-1}{J\cdot\sqrt{\bar{a}}}(\bar{a}\cdot\frac{\partial q}{\partial x}-s\cdot\frac{\partial q}{\partial h}) \qquad \ldots(18)$$

$$Nu_{ave}=\frac{1}{W}\int_0^W Nu_l\cdot dx \qquad \ldots(19)$$

The above integral was calculated using Simpson's rule 1/3 method.

To show the effect of the nano-fluids on heat transfer rate, we introduce a variable called Nusselt number ratio (NUR) with its definition given as:

$$NUR=\frac{Nu_{ave}|_{with\ nanofluids}}{Nu_{ave}|_{pure\ fluid}} \qquad \ldots(20)$$

If the value of NNR greater than 1 indicated that the heat transfer rate is enhanced on that fluid, whereas reduction of heat transfer is indicated when NUR is less than 1.

Results and Discussion

Results presented into two sections, the first section will focus on flow and temperature fields, which contents streamlines, isotherms for pure fluid and nano-fluids types. Another case of results represented the distribution of local Nusselt number on the heated wall, average nusselt number, and NUR factor.

Flow and Temperature Fields

Flow and temperature fields are simulated using streamlines and isotherms for selected parameters of nano-fluids types, nano-particles volume fraction, and geometry. Effects of Rayleigh number on streamlines and isotherms are presented in fig. (4) for Cu-water nano-fluid, AR=1., and PHI=0.2, visualization are given from Ra=104 to Ra=106. It can be seen from

figure that, for $Ra \le 10^5$ three vortices are formed for nano-fluid case (plotted by dashed lines) and two vortices are for pure fluid case (plotted by solid lines). This is due to different thermal physical properties in theses cases and to non uniform heating from below, so the heated flow moves up from the horizontal heated wall of the enclosure and impinges to the cold inclined wall. The first vortex is formed between heated horizontal wall and the inclined cooled wall of the triangular enclosure, which rotates in clockwise direction. Its shape and length are almost same in this range of Rayleigh number. The second vortex located between the heated wall and insulated wall which rotates in counterclockwise direction.

In this range of Rayleigh number ($Ra \le 10^5$) the difference between nano-fluid case and pure fluid case are the strong values of streamlines and a third vortex located in the top corner of the enclosure in nano-fluid case. Then, for $Ra = 10^6$ the two vortex are exist in the enclosure for nano-fluid and pure fluid cases, but the location and direction are opposite moreover to the strong convection will become here. These effects in heat transfer could be match on isotherms (right colum) in figure (4) where the isotherms are regular and uniform distribution in the enclosure for low Rayleigh number. Where the quasi-conduction heat transfer regime is formed clearly for low Rayleigh number, but if Rayleigh numbers increase the convection regime become strong and clear. Also, for high Rayleigh number the isotherms become non uniform and random due to increasing of energy exchange rates in the fluid. Generally, isotherms change and deform according to change in streamlines.

If nano-particles changed as shown in fig. (5) for Al_2O_3 and fig. (6) for TiO_2 the same behavior could be see for streamlines and isotherms with decreasing in values of absolute maximum streamlines according to the reduction in heat transfer due to the decreasing in the thermo-physical properties of Al_2O_3 and TiO_2 nano-particles comparing with Cu nano-particle.

Aspect ratio AR of the triangular enclosure is important parameter for flow and temperature fields. This changed from 0.5 to 2 along the present study. Thus, fig. (7) shows the effect of AR on streamlines (on the left) and isotherms (on the right) for Cu-water nano-fluid at $Ra=10^6$ and PHI=0.2. Two vortices are observed for AR=0.5, the right vortex rotates in clockwise direction while left one in counterclockwise direction. The separated line between them take place after mid point of the length of bottom wall of the enclosure due to non uniform heating from below and different boundaries about heated horizontal wall. These vortices are have an egg-shaped recirculation moreover to be strong flow strength became here in nano-fluid case comparing with pure fluid case.

For AR=1. , there are two vortices weak one on the right side and big vortex in the other side of the enclosure in pure fluid case, but in nano-fluid case this description could be changed where a small vortex located in the left side and big strong vortex located in the other side with high intensity of streamlines and strong flow strength. In AR=2., three vortices distributed in the enclosure with different direction and strength, on in the right side, left side, and on the top region of the enclosure. But in nano-fluid case, these vortices could grouping and become one strong vertex in the middle region of the enclosure. This phenomena at streamlines which effects on isotherms which are uniform nearly at AR=0.5 and become random and irregular in the enclosure If AR increase due to vortices and non uniform heating. This description could be see in fig. (8) and fig. (9) for

Al_2O_3, and TiO_2 nano-particles respectively, with decreasing in flow strength and special case in AR=1 for Al_2O_3 in fig. (8) where, three vortices in the enclosure comparing with the other cases.

Nusselt number and NUR factor

The changes in Nu_l for water based Cu, Al_2O_3, TiO_2 nano-particles at different Ra, AR, and PHI presented in figures (10), (11), and (12) respectively. In general for $Ra \le 10^5$, the distribution of Nu_l are parable and max. value of Nu_l located after mid point of the axis. If $Ra = 10^6$, the distribution will become fluctuation along the heated wall due to the circulation strength increases as a result of higher buoyancy force this results in an increase of the Nu_l moreover to strong heat exchange between the particles and base fluid . Fig. (13) presents the Nu_l distribution along the heated wall for different nano-particles and AR at Ra=10^5, and PHI=0.1 . Results show that, high Nu_l accurse at Cu, TiO_2, Al_2O_3, nano-particles respectively. Results show the important nano-fluid technology in engineering application. Fig. (14) shows the variation of Nu_{ave} with nano-particle volume fraction for different AR, Ra, and nano-particles type. Where, the Nu_{ave} increase with increase PHI for all cases, due to increase the heat exchange between the solid particles and based fluid for this range of PHI. Other results can be seen in fig. (15) for Nu_{ave} with nano-particle volume fraction, where as Ra increase the circulation strength increase as results of increasing in buoyancy force, the relation nearly is linear.

NUR factor are calculated to obtain the case of heat transfer enhancement could be happen, this results presented as a percentage values in table (2).

Conclusion

In these analysis, the results of the study of natural convection in triangular enclosure filled with nano-fluids with non uniform heating from bellow are presented for main parameters of interested as Ra, AR, nano-particles type, and nano-partical volume fraction. In view of the obtained results, following findings may be summarized:

1. The type of nano-fluid is a key factor for heat transfer enhancement. The high values are obtained when using Cu, TiO_2, and Al_2O_3 nano-particles respectively.
2. Flow strength and heat transfer rate are increasing generally in nano-fluid case comparing with pure fluid case.
3. NUR factor increase generally with Ra at constant PHI and increases with PHI at constant Ra.
4. Heat transfer is very weak at the left and top region in the enclosure when it compared with the right region.
5. It is observed that the aspect ratio of the enclosure is one of the most important on flow and heat transfer. Increasing the AR leads that to increase the flow strength and heat transfer rate.
6. Generally, for low Ra, the streamlines and isotherms are uniform due to quasi-conduction heat transfer regime where formed clearly but if Ra increase the convection heat transfer region become clear and streamlines and isotherms become non uniform and random.

NOMENCLATURE		
A,B,C,D, E	Transformation parameters.	
Al_2O_3	Alumina	
C_p	Specific heat at constant pressure	$kJ/kg.K$
Cu	Copper	
J	Jacobian	
g	Gravitational acceleration	m/s^2

H	Height of the enclosure	m
k	Thermal conductivity	$W/m^2 \cdot K$
Nu	Nusselt number	
PHI	Nano-particle volume fraction	
Pr	Prandtl number	
Ra	Rayleigh number	
T	Dimensional Temperature	k
TiO_2	Titanium oxide	
u, v	Dimensionless Velocity components	
W	Width of the enclosure	m
x, y	Dimensionless coordinates	
Greek symbols		
$\overline{a}, g, s$	Transformation functions	
a	Thermal diffusivity	m^2/s
b	Thermal expansion coefficient	$1/K$
x, h	curvilinear coordinates	
q	Dimensionless temperature	
Ψ	Dimensionless stream function	
y	Dimensional stream function	m^2/s
w	Dimensional vorticity	$1/s$
Ω	Dimensionless vorticity	
r	Density	kg/m^3
m	Dynamic viscosity	$N \cdot s/m^2$
Subscripts		
ave	Average value	
c	cooled	
l	Local	
f	Fluid	
nf	Nano-fluid	
h	Hot	
s	Solid	
w	Wall	
p	Particle	
Superscripts		
'	Dimension quantity	

References

[1] Cho, S.U.S.;"**Enhancing Thermal Conductivity of Fluids with Nanoparticles**", in: D. A. signer, H.P. wang (Eds), Developments and Applications of Non-Newtonian Flows, FED, vol.231/MD-vol.66, ASME, New York, 1995, pp. 99-105.

[2] Yanjiao Li, Jing'en Z., Simon T., Eric S., and Shengqi X.;"**A Review on Development of Nanofluid Preparation and Characterization**", Powder Technology Journals, vol. 196, 2009, pp. 89-101.

[3] Eiyad A.N.;" **Effects of Variable Viscosity and Thermal Conductivity of Al_2O_3-water nanofluid on Heat Transfer Enhancement in Natural Convection** ", Int. Journal of Heat and Fluid Flow, 2009.

[4] Eiyad A.N., and Hakan F.O.;" **Effects of Inclination Angle on Natural Convection in Enclosures Filled with Cu-water Nanofluid**", Int. Journal of Heat and Fluid Flow, 2009.

[5] Eiyad A.N., Ziyad M., Hakan F.O., and Antonio C.;" **Effect of Nanofluid Variable Properties on Natural Convection in Enclosures**", Int. Journal of Thermal Sciences, 2009.

[6] Elif B.O.;" **Natural Convection of Water-based Nanofluids in an Inclined Enclosure with a Heat Source** ", Int. Journal of Thermal Sciences, vol. 48, 2009,pp. 2063-2073.

[7] Hakan F.O., and Eiyad A.N.;" **Numerical Study of Natural Convection in Partially Heated Rectangular Enclosure Filled with Nanofluids**", Int. Journal of Heat and Fluid Flow, vol. 29, 2008, pp. 1326-1336.

[8] Eiyad A.N, Masoud Z., and Hijazi Ai;" **Natural Convection Heat Transfer Enhancement in Horizontal Concentric Annuli Using Nanofluids**", Int. Communication in Heat and Mass Transfer, vol. 35,2008,pp. 657-665.

[9] Ghasemi B., and Aminossadati S.M.;" **Periodic Natural Convection in a Nanofluid-Filled enclosure with Oscillating Heat Flux**", Int. Journal of Thermal Sciences, 2009.

[10] Mansour R. Ben, Galanis N., and Nguyen C.T.;" **Effect of Uncertainties in Physical Properties on Forced Convection Heat Transfer with Nanofluids**", Applied Thermal Eng., vol. 27(1),2007,pp. 240-249.

[11] Akbari M., Behzadmehr A., and Shahraki Fi;" **Fully Developed Mixed Convection in Horizontal and Inclined Tubes with Uniform Heat Flux Using Nanofluid**", Int. Journal of Heat and Fluid Flow, vol. 29, 2008, pp. 545-556.

[12] Hwang K.S., Jong S.P., and Choi S.U.S.," **Flow and Convection Heat Transfer Characteristics of Water Based Al_2O_3 Nanofluids in Fully Developed Laminar Flow Regime**", Int. Journal of Heat and Mass Transfer, vol. 52, 2009, pp. 193-199.

[13] Ho C.J., Wei L.C., and Li Z.W.," **An Experimental Investigation of Forced Convection Cooling Performance of a Microchannel Heat Sink with Al_2O_3-water Nanofluid**", Applied Thermal Eng., 2009**.**

[14] Heris S.Z., Esfahany M.N., Etemad S.GH.;" **Experimental Investigation of Convective Heat Transfer of Al_2O_3-water Nanofluid in Circular Tube**", Int. Journal of Heat and Fluid Flow, vol. 28, 2007, pp. 203-210.

[15] Mirmasoumi S., Behzadmehr A.;" **Effect of Nanoparticles Mean Diameter on Mixed Convection Heat Transfer of a Nanofluid in a Horizontal Tube**", Int. Journal of Heat and Fluid Flow, vol. 29, 2008, pp. 557-566.

[16] Akbrinia A., Behzadmehr A.;' **Numerical Study of Laminar Mixed Convection of a Nanofluid in Horizontal Curved Tubes**", Applied Thermal Eng., vol. 27,2007, pp. 1327-1337.

[17] Eiyad A.N," **Application of Nanofluids for Heat Transfer Enhancement of Separated Flows Encountered in a Backward Facing Step**", Int. Journal of Heat and Fluid Flow, vol. 29, 2008, pp. 242-249.

[18] Khanafer K., Vafai K., and Lightstone M., " **Bouyancy-driven Heat Transfer Enhancement in a Two-Dimensional Enclosure Utilizing Nanofluids**", Int. Journal Heat Mass Transfer, vol. 46, 2003, pp. 3639-3653.

[19] Brinkman H.C.," **The Viscosity of Concentrated Suspensions and Solutions**", Journal of Chem. Phys., 20, 1952, pp. 571-581.

Table (1) Thermo-physical properties of fluid and nano-particles.

Physical properties	water	Cu	Al_2O_3	TiO_2
C_p (J/kg.K)	**4179**	**385**	**765**	**686.2**
r (kg/m^3)	**997.1**	**8933**	**3970**	**4250**
K (W/m.K)	**0.613**	**400**	**40**	**8.9538**
$a \times 10^7$ (m^2/s)	**1.47**	**1163.1**	**131.7**	**30.7**
$b \times 10^{-5}$(1/K)	**21**	**1.67**	**0.85**	**0.9**

Table (2) Percentage values (%) of NUR factor for different cases.

PHI	*AR*=0.5		
	Rayleigh number (Ra)		
	10^4	10^5	10^6
Cu-water nanofluid			
0.1	6	10	7.5
0.2	12.6	16.5	13.8
0.4	17.6	22.48	20.6
TiO_2-water nanofluid			
0.1	4.3	5.77	5.4
0.2	10.8	12.2	8
0.4	13	16.3	12.2
Al_2O_3-water nanofluid			
0.1	1.7	2.1	1.33
0.2	5.5	6.5	5.88
0.4	7.2	12	7.2

Table (2) cont.

PHI	*AR*=1.		
	Rayleigh number (Ra)		
	10^4	10^5	10^6
Cu-water nanofluid			
0.1	12	21	6.4
0.2	23.9	35.8	10
0.4	32.7	40.7	15.2
TiO_2-water nanofluid			
0.1	5.9	10.6	2.9
0.2	11.8	18.1	8.6
0.4	20.8	14.4	11.2
Al_2O_3-water nanofluid			
0.1	2.9	1.7	1.3
0.2	5.8	11.7	2.5
0.4	13.8	14.7	6.9
PHI	*AR*=2.		
	Rayleigh number (Ra)		
	10^4	10^5	10^6
Cu-water nanofluid			
0.1	15.8	16.1	5.2
0.2	32	23.7	9.1
0.4	44	22.2	16.1
TiO_2-water nanofluid			
0.1	7.5	4.9	1.3
0.2	15.4	10.3	5.7
0.4	27.4	14	9.5
Al_2O_3-water nanofluid			
0.1	3.3	2.7	0.4
0.2	11.3	6.6	2.9
0.4	19.2	11.3	7.2

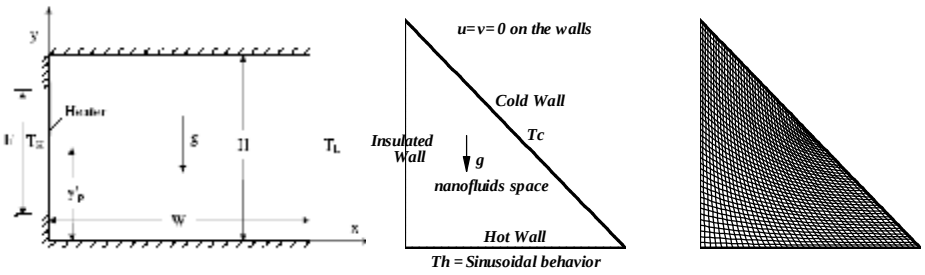

Figure. (1) Sketch of the validation problem geometry and coordinates (A), with present problem geometry (B), and grid generation behavior in this study (C)

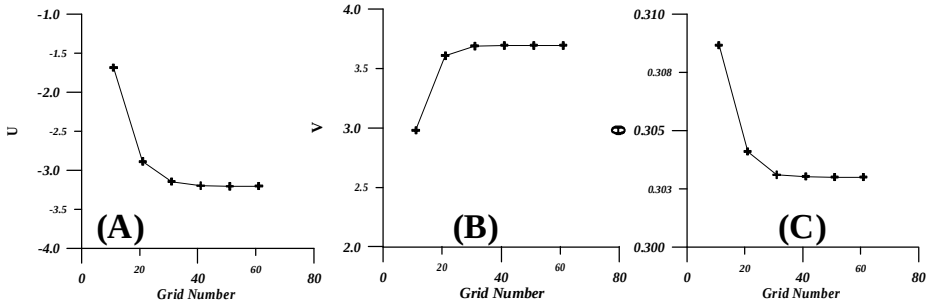

Figure (2) Grid Size Study for point at the middle of the enclosure at $Ra=10^5$, AR=1, PHI=0.

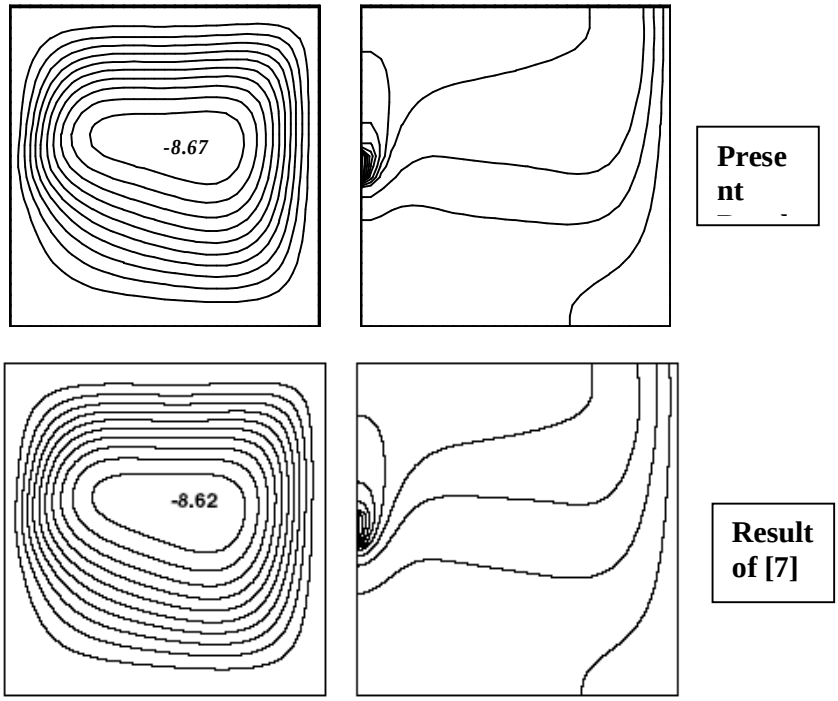

Figure (3) Streamlines (on the left) and isotherms (on the right) for Cu-water nanofluids for validation case with $Ra = 10^5$, $y_p = 0.5$, AR = 1, h = 0.1, PHI = 0.1.

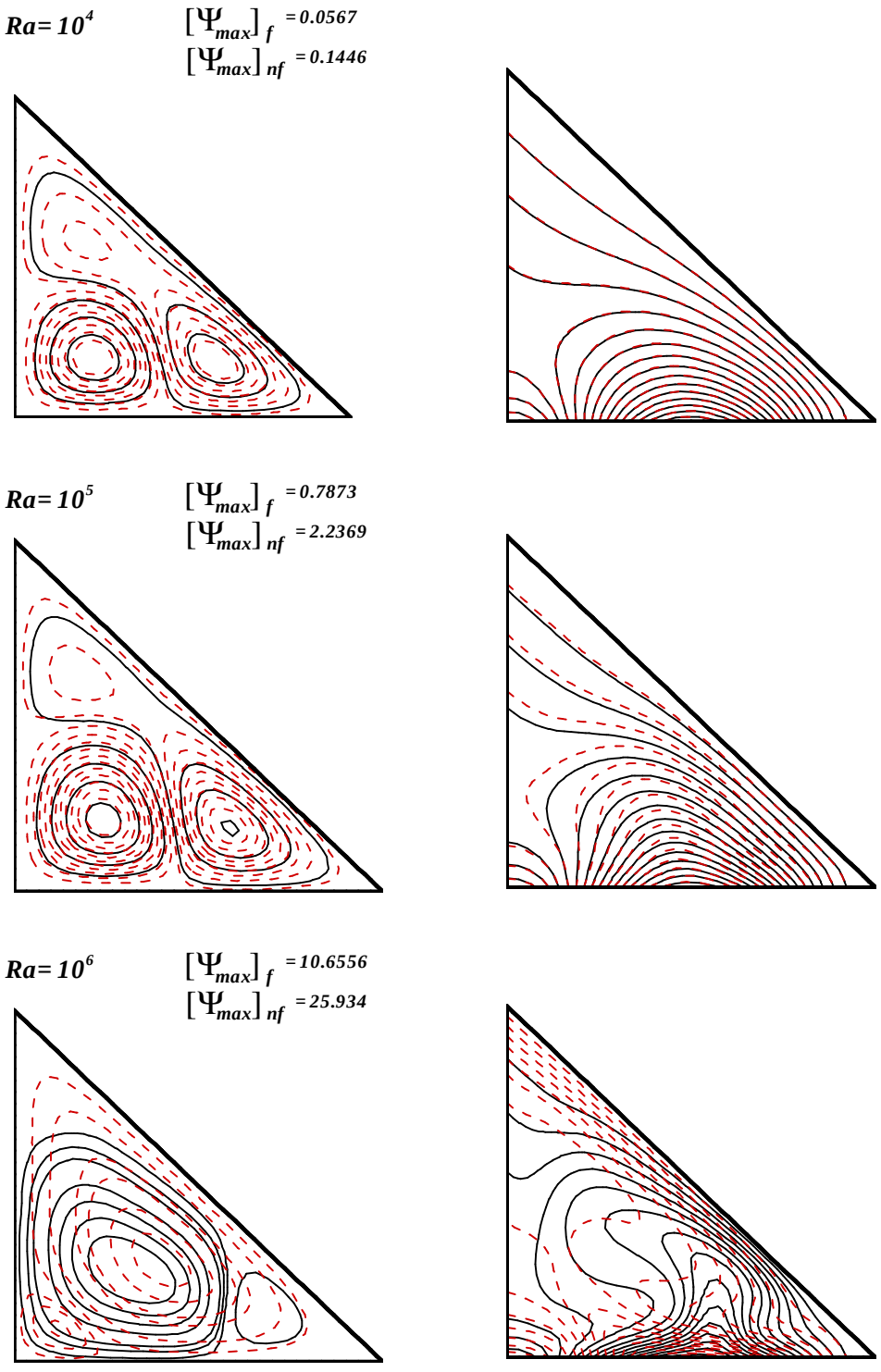

Figure (4) Streamlines (on the left) and Isotherms (on the right) for Cu-water nanofluid (- - - -), pure fluid (——), with AR=1. and PHI=0.2.

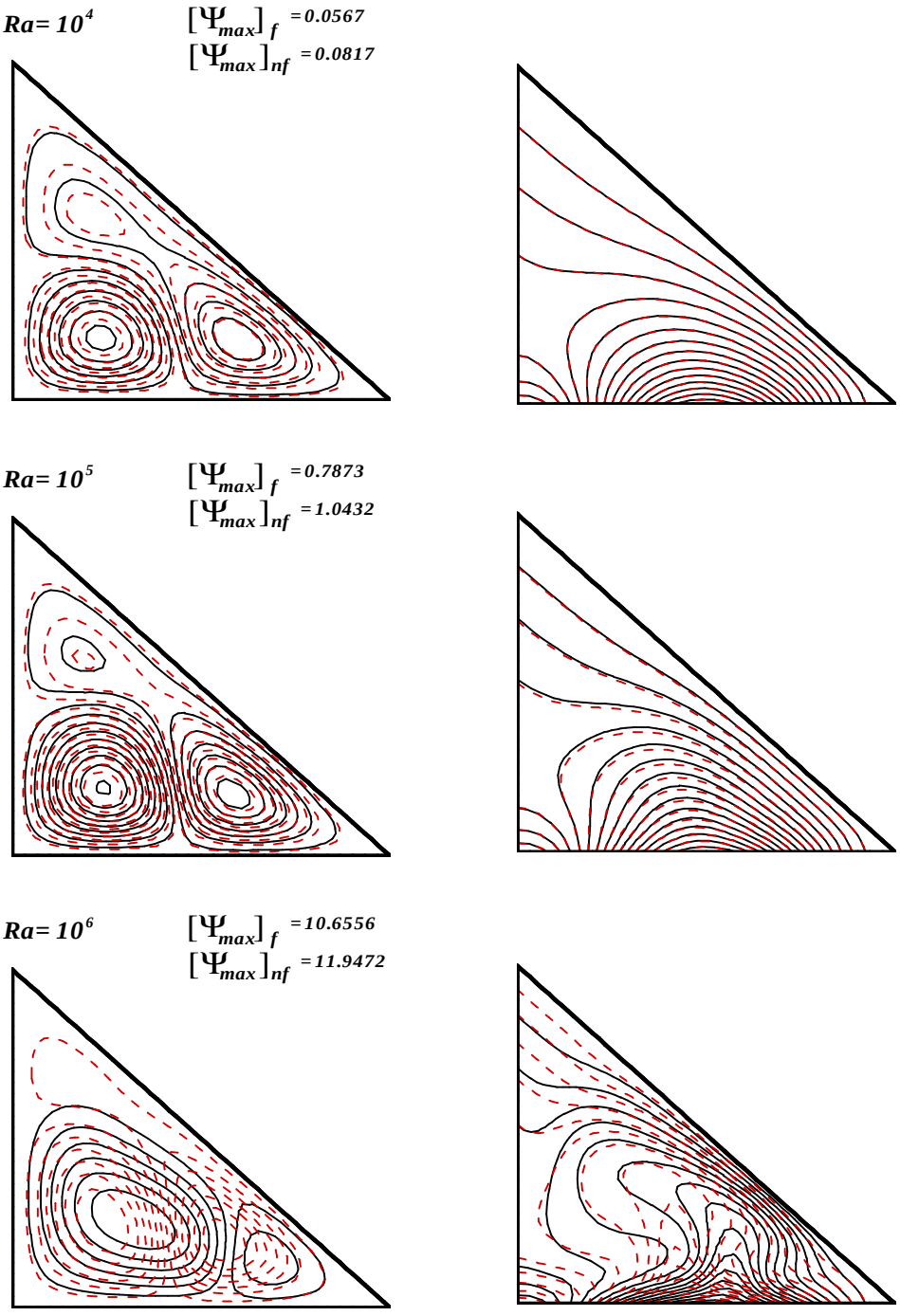

Figure (5) Streamlines (on the left) and Isotherms (on the right) for Al_2O_3-water nanofluid (- - - -), pure fluid (——), with AR=1. and PHI=0.2.

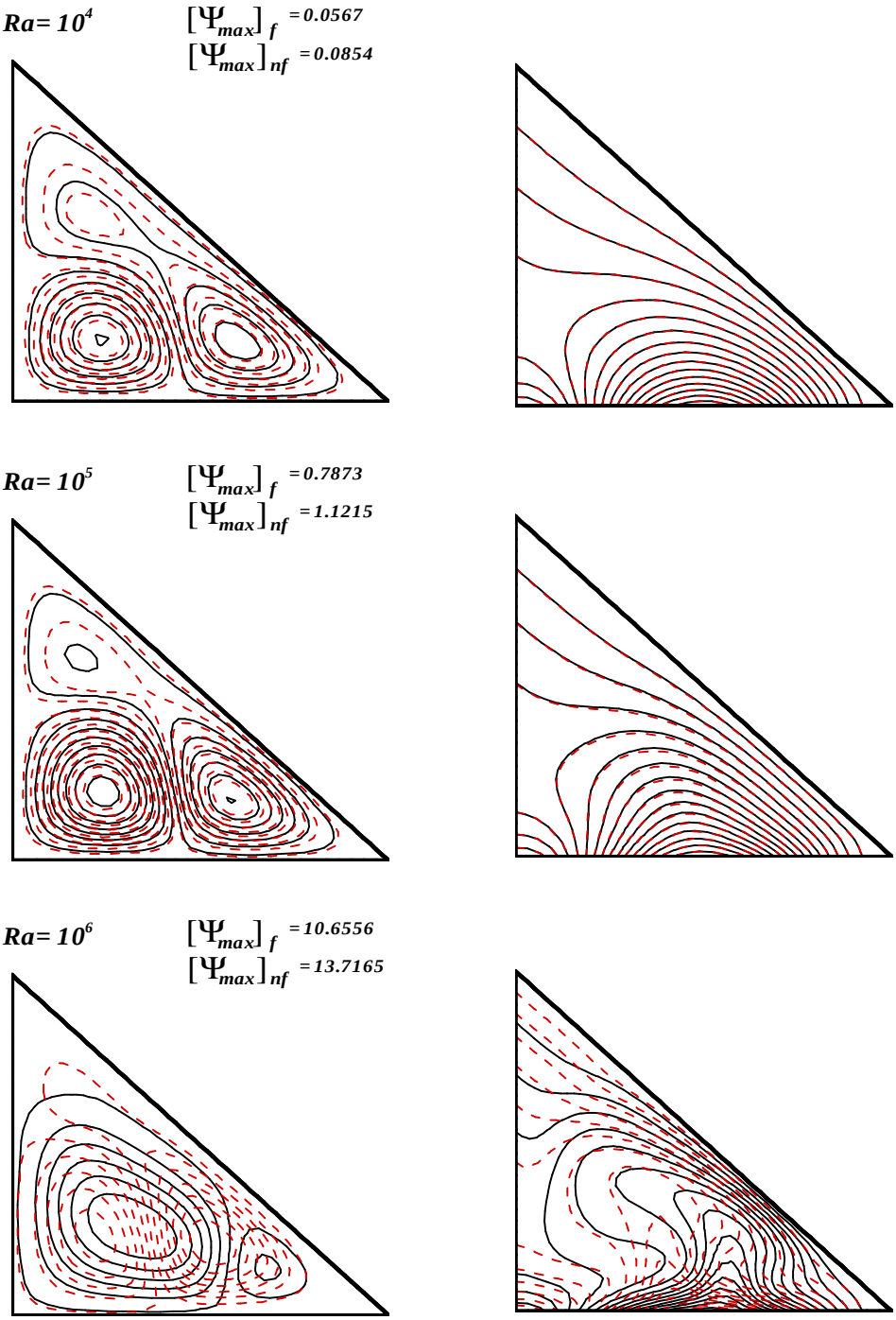

Figure (6) Streamlines (on the left) and Isotherms (on the right) for TiO_2-water nanofluid (- - - -), pure fluid (——), with AR=1. and PHI=0.2.

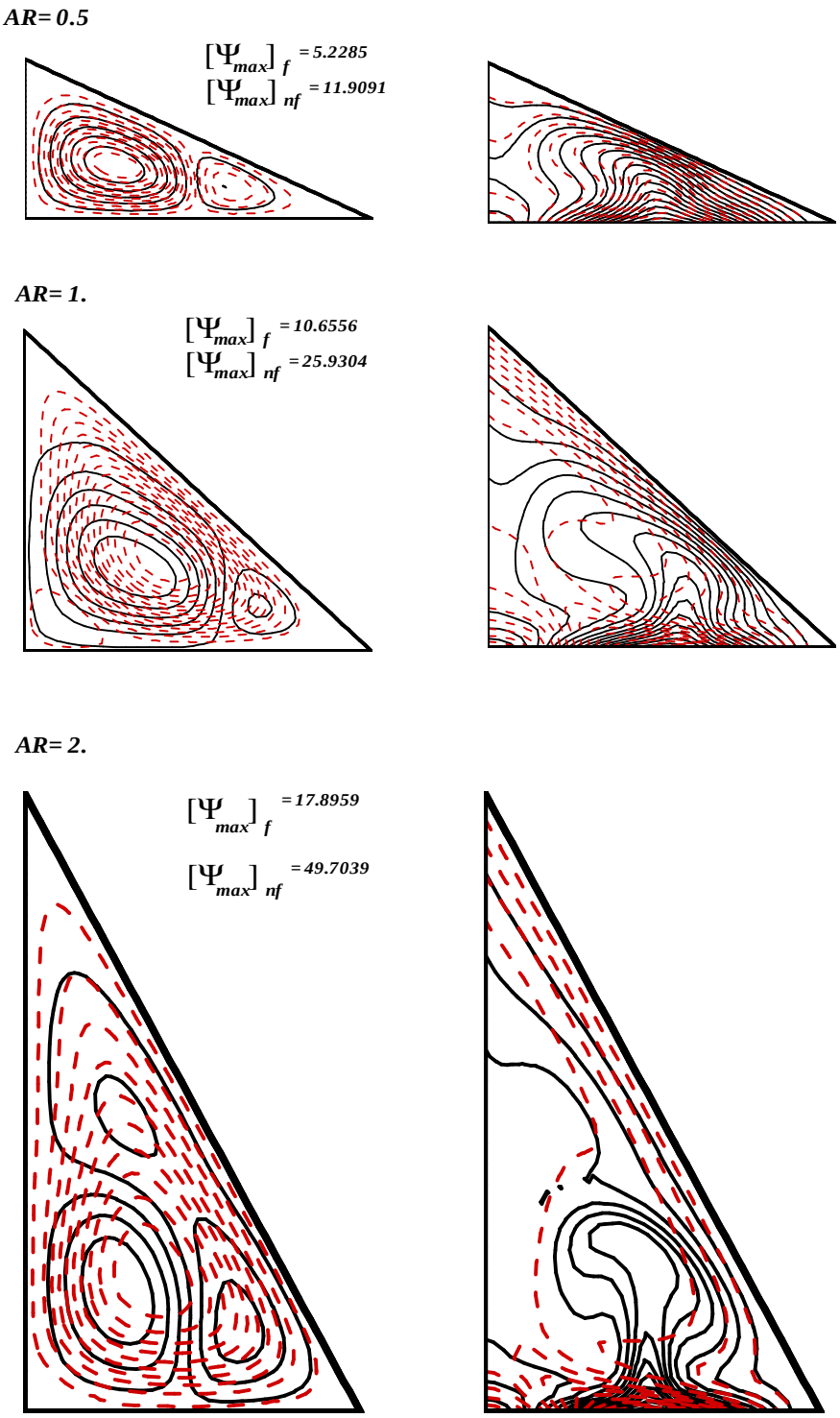

Figure (7) Streamlines (on the left) and Isotherms (on the right) for Cu-water nanofluid (- - - -), pure fluid (——), with Ra=10^6. and PHI=0.2.

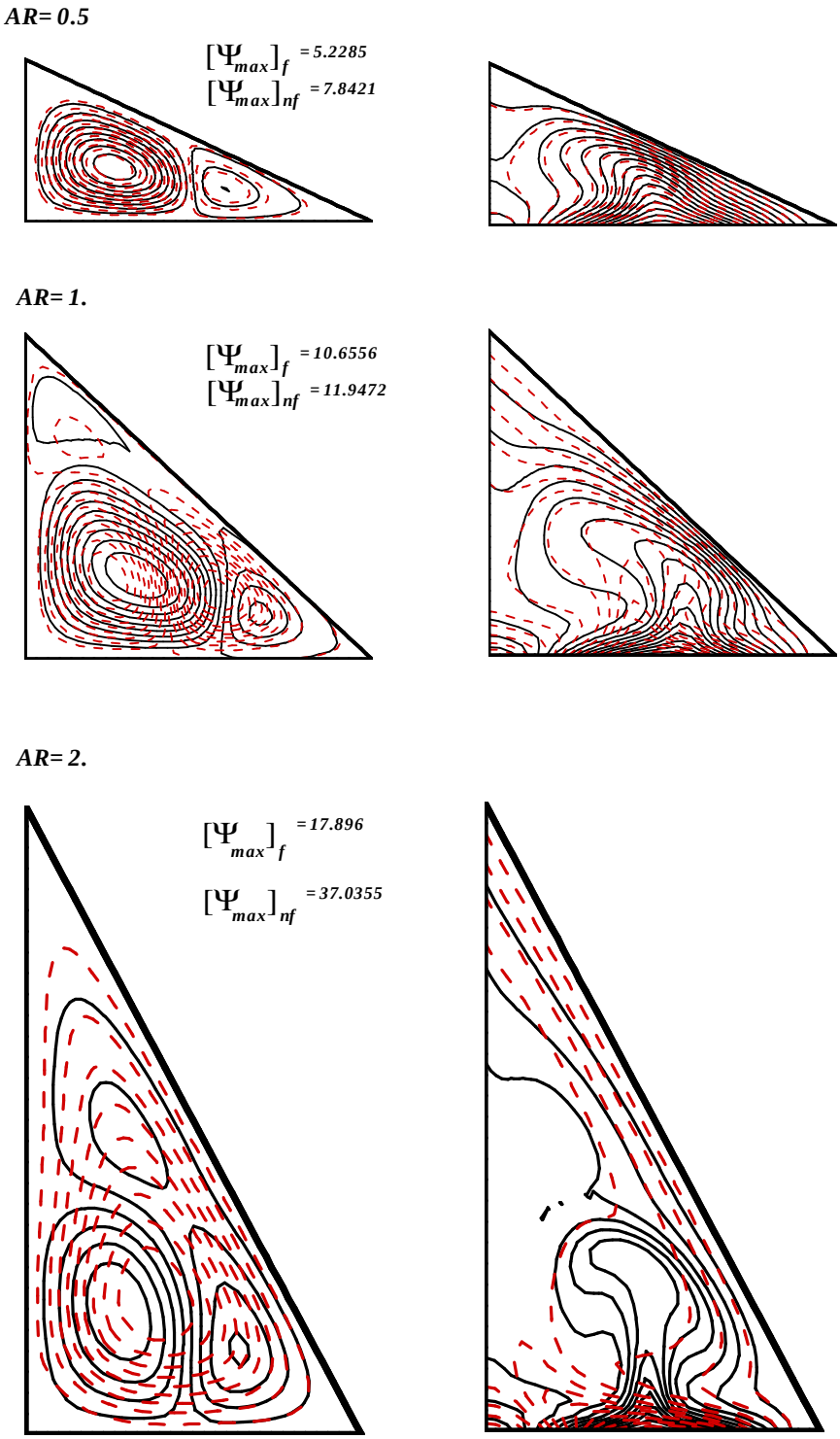

Figure (8) Streamlines (on the left) and Isotherms (on the right) for Al_2O_3-water nanofluid (- - - -), pure fluid (——), with Ra=10^6. and PHI=0.2.

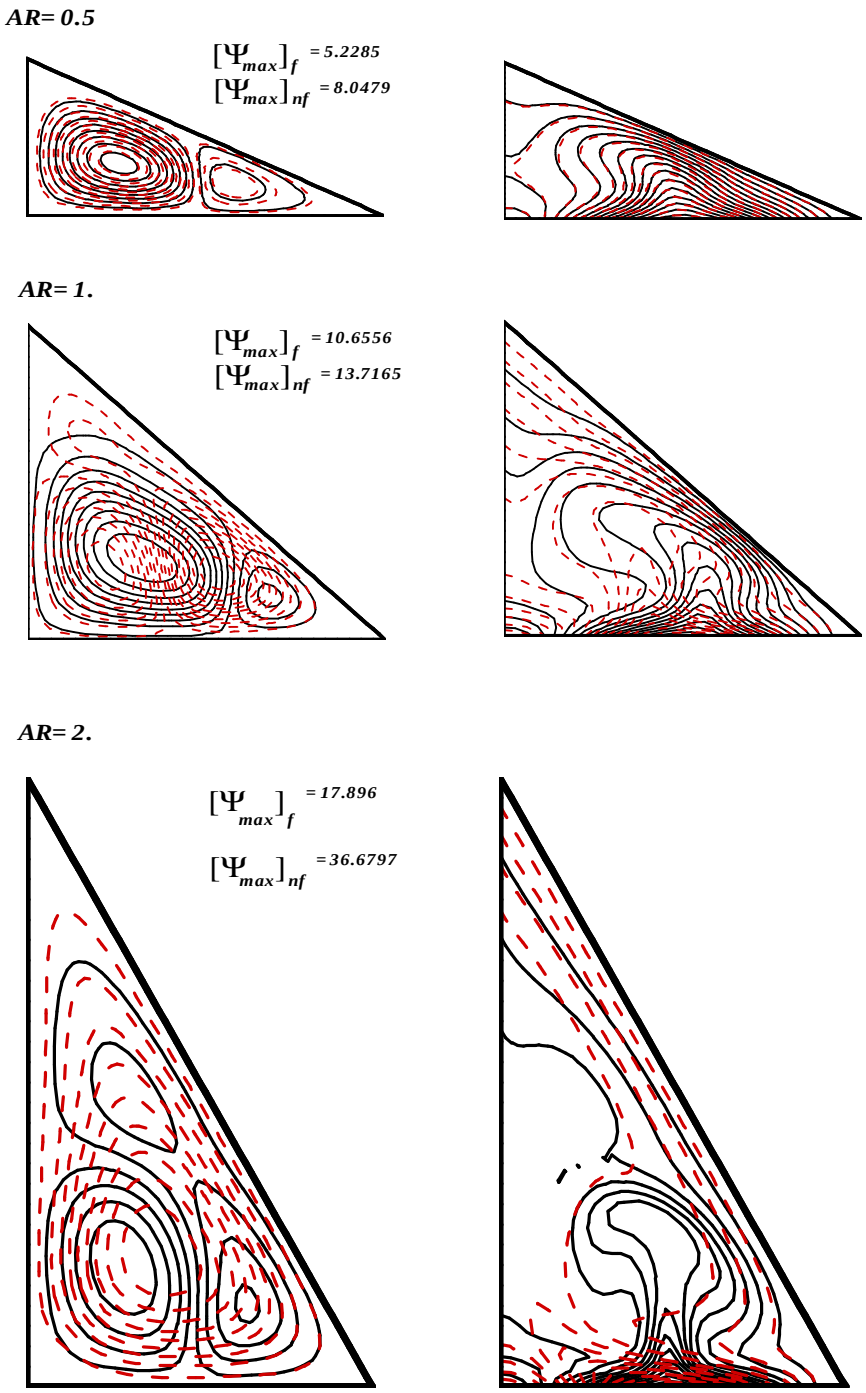

Figure (9) Streamlines (on the left) and Isotherms (on the right) for TiO_2-water nanofluid (- - - -), pure fluid (——), with Ra=10^6. and PHI=0.2.

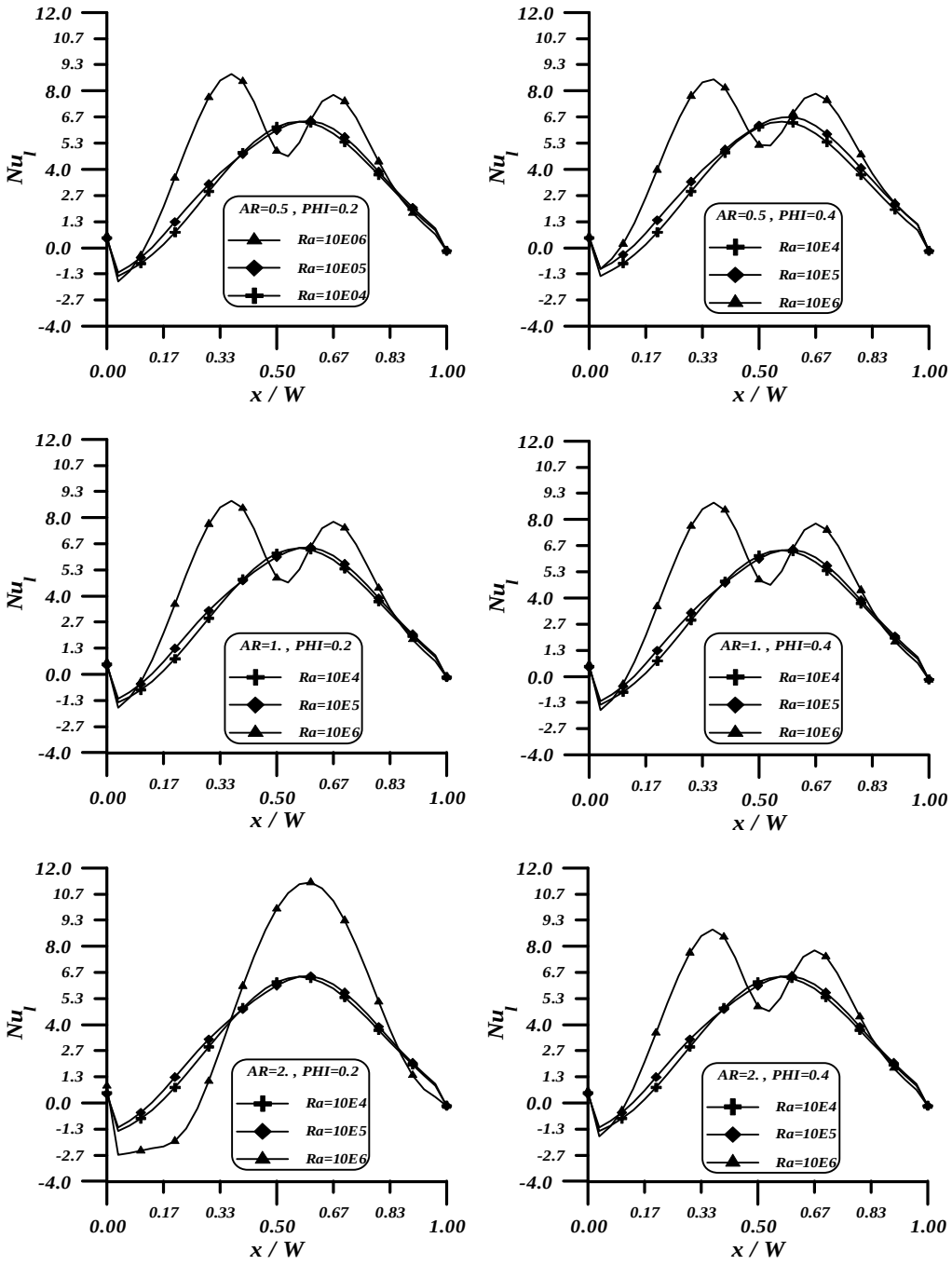

Figure (10) Variation of local Nusselt number along the heated wall for different aspect ratio, and Rayleigh number for Cu-water nanofluid.
Left side: PHI=0.2 , Right side: PHI=0.4

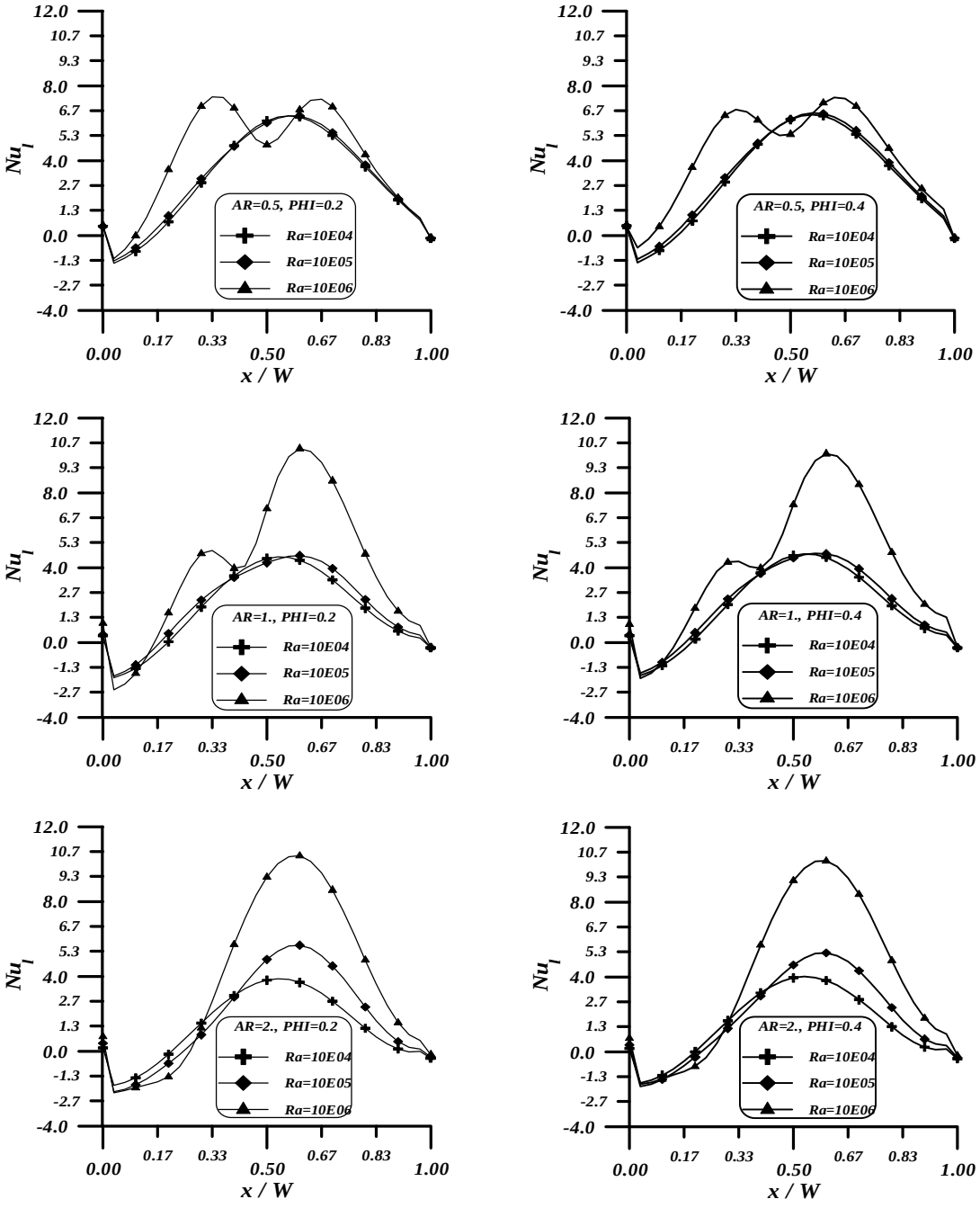

Figure (11) Variation of local Nusselt number along the heated wall for different aspect ratio, and Rayleigh number for TiO_2-water nanofluid
Left side: PHI=0.2 , Right side: PHI=0.4

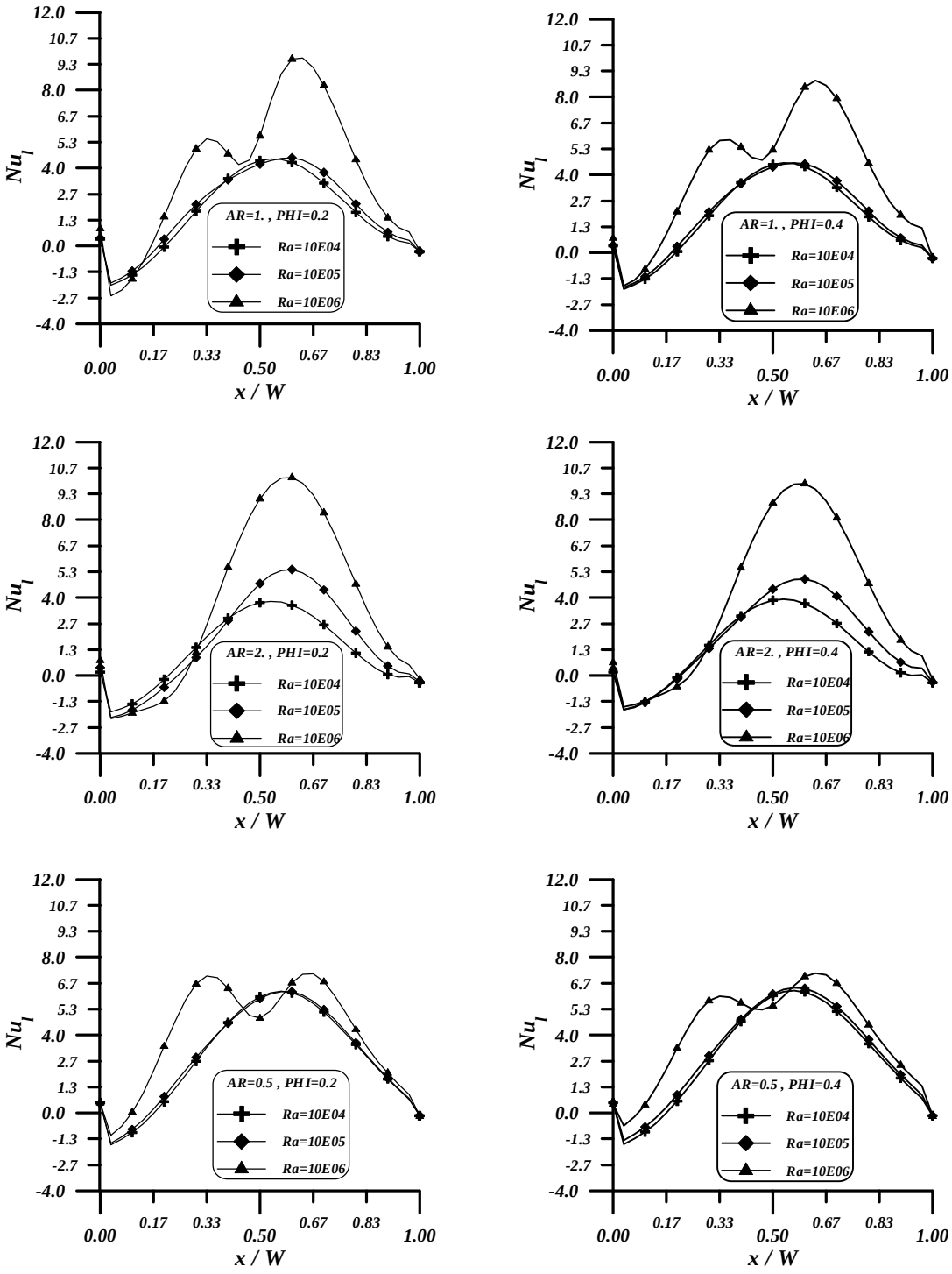

Figure (12) Variation of local Nusselt number along the heated wall for different aspect ratio, and Rayleigh number for Al_2O_3-water nanofluid
Left side: PHI=0.2 , Right side: PHI=0.4

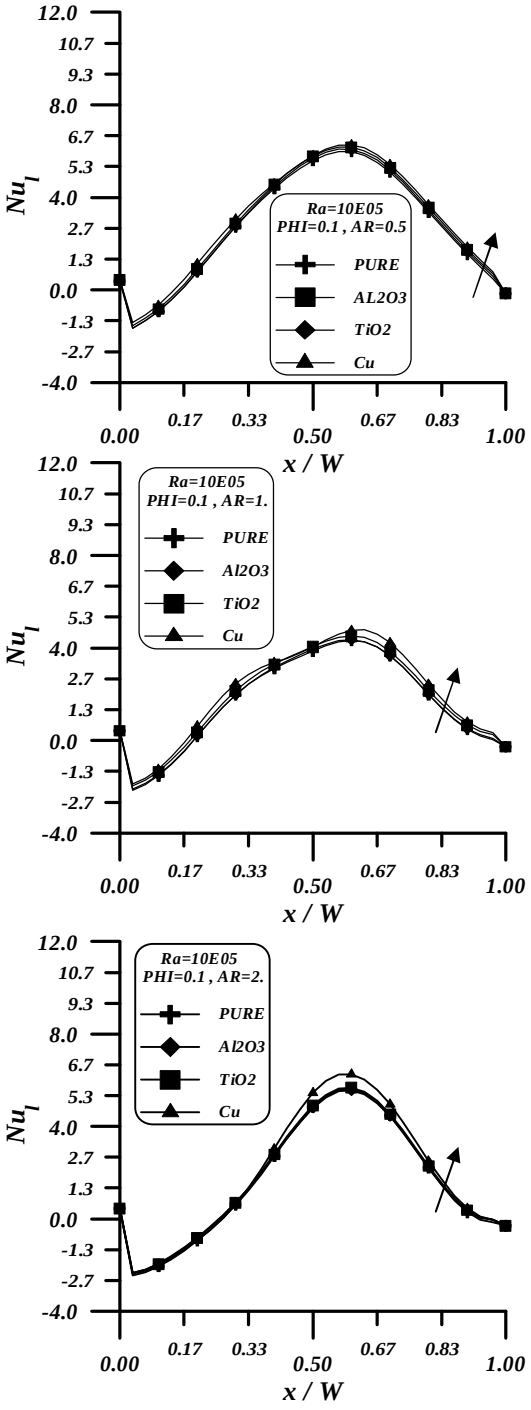

Figure (13) Variation of local Nusselt number along the heated wall for different aspect ratio, and Nanoparticles type for Ra=10^5, PHI=0.1

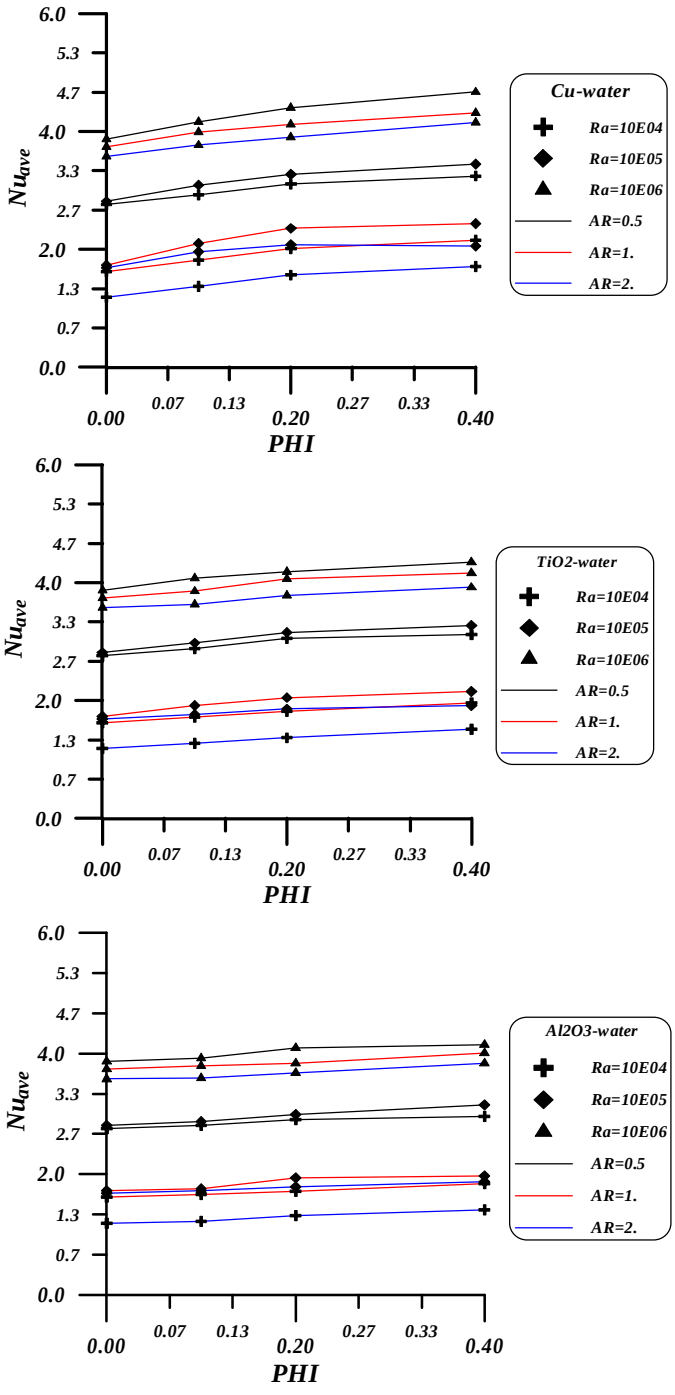

Figure (14) Variation of average Nusselt number with nanoparticles volume fraction for different aspect ratio, Rayleigh number and Nanoparticles type.

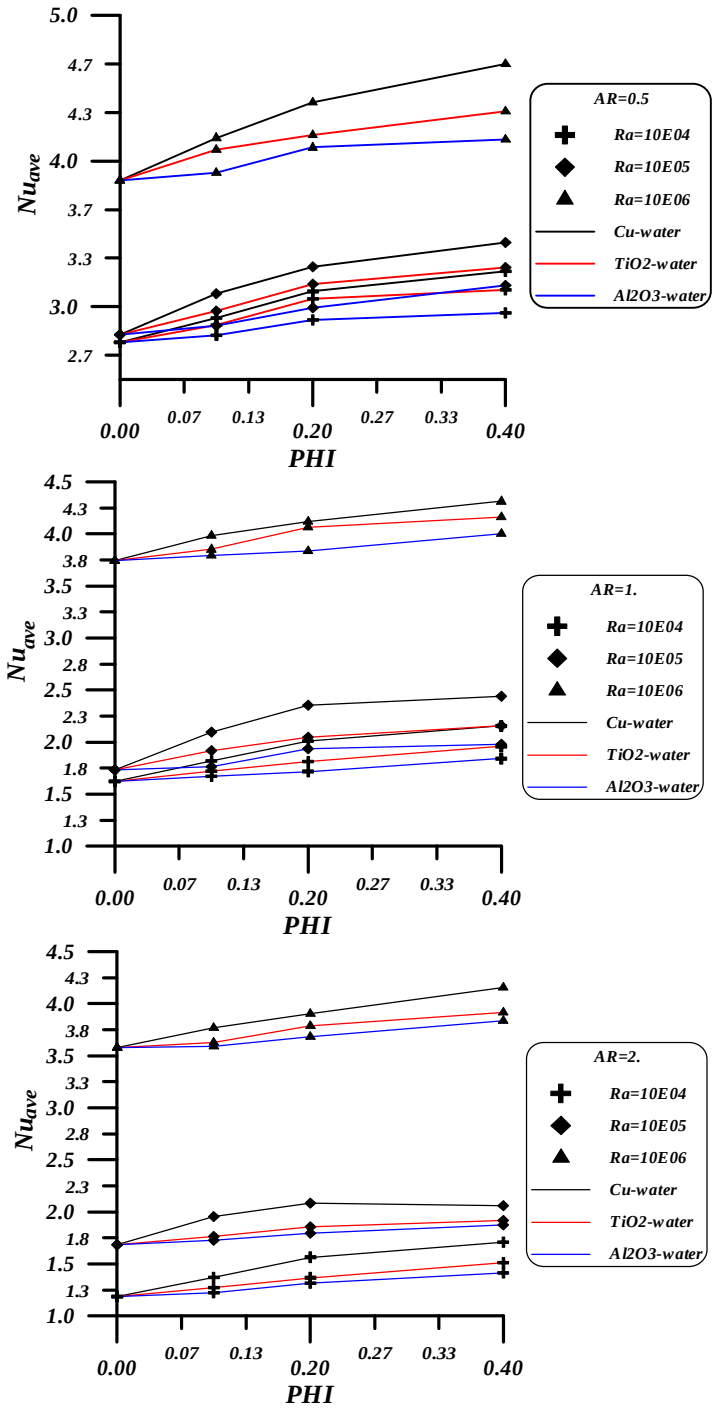

Figure (15) Variation of average Nusselt number with nanoparticles volume fraction for different aspect ratio, Rayleigh number and Nanoparticles type.